

See discussions, stats, and author profiles for this publication at: <https://www.researchgate.net/publication/231370351>

Concentration of Apple Juice by Reverse Osmosis at Laboratory and Pilot-Plant Scales

ARTICLE *in* INDUSTRIAL & ENGINEERING CHEMISTRY RESEARCH · NOVEMBER 2002

Impact Factor: 2.59 · DOI: 10.1021/ie020013g

CITATIONS

3

READS

60

4 AUTHORS, INCLUDING:



Silvia Álvarez

Universitat Politècnica de València

60 PUBLICATIONS 888 CITATIONS

SEE PROFILE



Francisco Riera

University of Oviedo

72 PUBLICATIONS 885 CITATIONS

SEE PROFILE

Concentration of Apple Juice by Reverse Osmosis at Laboratory and Pilot-Plant Scales

Silvia Álvarez, Francisco A. Riera,* Ricardo Álvarez, and José Coca

Department of Chemical Engineering and Environmental Technology, University of Oviedo, C/Julián Clavería 8, 33 006 Oviedo, Spain

The aim of this work was to predict the rejection of aroma compounds and permeate flux during the reverse osmosis concentration of apple juice at laboratory and pilot-plant scales. For the concentration, the MSCB2521 R99 and MSCE 4040 R99 spiral wound membranes (Separex, SpA, Biella, Italy) were used at laboratory and pilot-plant scales, respectively. The *preferential sorption-capillary flow* model was considered for the calculations. Experiments were performed at different transmembrane pressures (1.5–7.0 MPa), feed flows (200–600 L/h at laboratory scale and 4200 L/h at pilot-plant scale), temperatures (20–30 °C), and concentrations (10.0–22.7 °Brix). Good agreement between experimental and estimated data was observed for most of the aroma compounds and operating conditions used. When working at 7.0 MPa transmembrane pressure, 4200 L/h feed flow, and 25 °C temperature, concentrations higher than 22 °Brix can be reached with high permeate fluxes (higher than 25 L/h·m²) and high aroma retention (higher than 80% for most of the compounds).

1. Introduction

Conventional methods for producing fruit juices involve evaporation to concentrate the juice, which requires high temperatures and energy consumption. Part of the constituents are removed with the water vapor, and heat-induced changes can be observed in the product. Reverse osmosis (RO) is a membrane process of increasing interest in the food industry. It can be used to preconcentrate solutions, thus avoiding high temperatures. Therefore, minimum thermal damage is caused. Other advantages include lower capital and operating costs.^{1–3}

The success of RO for fruit juice concentration depends on an adequate retention of flavor components which may permeate the membrane.⁴ Merson and Morgan⁵ concluded that the major factor concerning the quality of the final products is the retention of flavor components because these affect the organoleptic properties such as odor and flavor. Retention of these components during the RO process is related to the types of membranes and the operating conditions used.

Apple juice aroma is caused by the blend of many compounds rather than the presence of one particular component. Three groups of compounds can be found in apple flavors: esters, aldehydes, and alcohols, with esters being reported as the most important ones. The major compounds thought to be responsible for apple flavor are ethyl butanoate, ethyl-2-methyl butanoate, *trans*-2-hexenal, and hexanal. Some authors have correlated the quality of juice flavors negatively with the presence of ethanol and ethyl acetate.^{6,7}

Several works have been published on the concentration of fruit juices by RO in the past few years.^{1,5,8–11} These papers paid special attention to the measurement of permeate flux using different types of membranes and operating conditions with only a few also measuring flavor retention. Polyamide (PA) membranes were found

to perform better in terms of both flux and flavor retention than cellulose acetate (CA) membranes. The modeling perspective has received less attention.

Several theoretical models have been proposed to predict solute and solvent flux through RO membranes.¹² The *preferential sorption-capillary flow* model was developed by Sourirajan and co-workers^{13,14} and has been applied to a mixture of D-glucose and D,L-malic acid,¹⁵ as well as mixtures of volatile organic compounds in aqueous solutions.^{16,17} In a previous paper by the authors,¹⁸ this mathematical model was satisfactorily used to predict permeate flux and aroma compounds retention when concentrating artificial solutions simulating apple juice, composed of glucose and apple juice aroma compounds. There is, however, little research on the application of these models to predict permeate and solute flux during the concentration of real multisolute food solutions, because there is little information about the physicochemical properties of such solutions. There are several correlations in the literature to estimate solution properties.^{19–21} The accuracy of the data predicted by the model depends greatly on the accuracy of the correlations used.

This work intends to study the *preferential sorption-capillary flow* model to predict the results obtained at laboratory and pilot-plant scales when concentrating real apple juice.

2. Materials and Methods

2.1. Feed Solutions. The apple juice used as the feed was prepared from 72 °Brix concentrated apple juice supplied by the apple processing company Valle, Ballina and Fernández, S.A. (Villaviciosa, Spain), by adding distilled water. The concentration of the feed solution prepared was 10.5 ± 0.5 °Brix for all of the experiments. Because this concentrated juice had previously been deodorized, apple juice aroma was added afterward. The composition of the final feed is indicated in Table 1.

2.2. Equipment. The experiments performed at laboratory scale were carried out in a RO setup designed

* Corresponding author. Tel.: + 34 8 5103436. Fax: + 34 8 5103434. E-mail: FAR@sauron.quimica.uniovi.es.

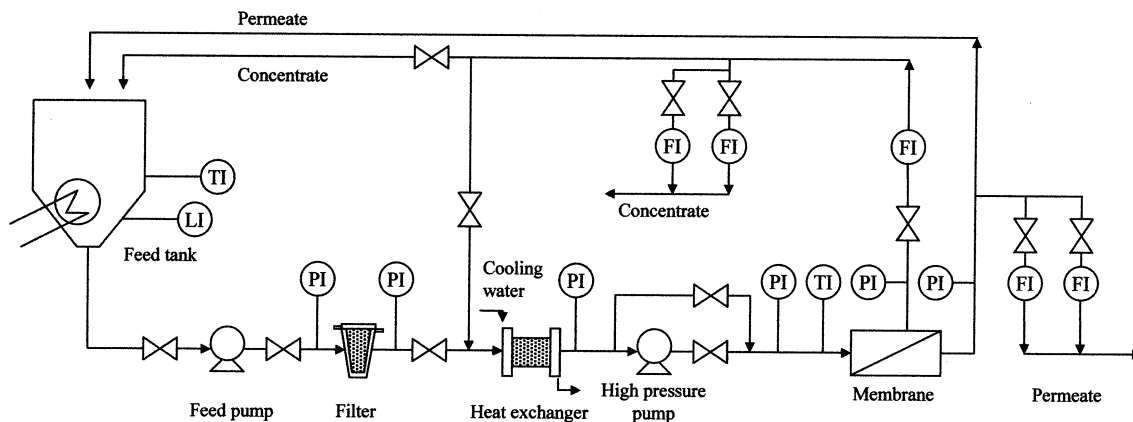


Figure 1. Diagram of the RO pilot unit.

Table 1. Composition of the apple juice used as feed

compound	concn (g/L)	mol wt
sucrose	12.16	342
glucose	24.84	180
fructose	61.33	180
malic acid	3.90	134
sorbitol	3.35	182

aroma compound	concn (ppm)	mol wt
ethyl acetate	50	88.11
ethyl butanoate	15	116.16
ethyl-2-methyl butanoate	7	130.19
isopentyl acetate	17	130.19
hexyl acetate	10	144.22
<i>trans</i> -2-hexenal	70	98.14
hexanal	15	100.2
isobutanol	20	74.12
butanol	20	74.12
isopentanol	15	88.15
hexanol	30	102.18
apple juice concn	10.5 °Brix	

Table 2. Manufacturer's Specifications for the Membrane Modules

	model	
	MSCB 2521 R99	MSCE 4040 R99
active surface (m ²)	1.0	6.0
membrane length (mm)	440	984
hydraulic diameter (mm)	0.96	0.93
spacer thickness (mm)	0.7	0.7
spacer porosity	0.908	0.908
max operating pressure (MPa)	4.2	7.0
max operating temperature (°C)	50	50
pH range		
continuous operation	4–11	4–11
during cleaning	2–12	2–12

at the University of Oviedo. The main components of the RO system are a 26 L feed tank, a CAT piston pump (model 311, 5.5 HP, Minneapolis, MN) with a maximum velocity of 2.95 m/s and an operating pressure of up to 5.5 MPa, a MSCB 2521 R99 spiral wound membrane module supplied by Separeem Spa. (Biella, Italy), a rotameter located in the retentate line, and a temperature and pressure control system. The RO module consists of a spiral wound aromatic polyamide membrane with a total effective area of 1.03 m² whose characteristics are shown in Table 2.

The equipment used at pilot-plant scale was designed by Separeem Spa. A diagram of the setup is shown in Figure 1. This consisted of a stainless steel feed tank of 500 L volume equipped with level and temperature

measures and a heating system, a centrifuge feed pump (CSF INOX, CIC–CLC series, Montecchio Emilia, Italy), a high-pressure volumetric recirculation pump (Bono Netro, Ronet 6000 series, Netro, Italy), a prefilter placed immediately after the feed pump, five rotameters to measure feed, permeate, and retentate flow, six manometers to measure the pressure at different points of the installation, a plate and frame heat exchanger, a control board, and a vessel for housing a RO spiral wound membrane. The equipment was also provided with temperature, pressure, and feed tank level control systems. The RO membrane module (MSCE 4040 R99) used was supplied by Separeem Spa. It consisted of a spiral wound membrane with a total effective area of 6.0 m², which was manufactured from the same PA as the laboratory-scale MSCB 2521 R99 membrane. The manufacturer's specifications for both membrane modules are shown in Table 2.

Retentate was recycled back to the feed tank in all of the experiments, while permeate was recirculated in experiments where the concentration was kept constant and removed from the equipment in those assays in which concentration was increased. Experiments at laboratory scale were performed at pressures from 1.5 to 3.5 MPa, temperatures from 20 to 30 °C, and feed flows between 200 and 600 L/h, while experiments at pilot-plant scale were carried out at 2.5 and 7.0 MPa transmembrane pressures (TMPs), a temperature of 25 °C, and a feed flow of 4200 L/h.

Both devices were cleaned in situ. The laboratory system was cleaned with a 0.2% (w/w) commercial P3 Ultrasil 10 (Henkel Ibérica, Barcelona, Spain) solution for 30 min at a temperature of 35–40 °C and rinsed with distilled water for about 15–20 min. The pilot-plant scale system was cleaned with a 1.5% (v/v) commercial P3 Ultrasil 91 solution for 120 min at a temperature of 40 °C and afterward with a 1.0% (w/w) commercial P3 Ultrasil 75 solution for 30 min at room temperature. Rinsing with tap water for 30 min was performed before and after each cleaning step. The flux of distilled water at a TMP of 1.5 MPa and a temperature of 25 °C was measured before each experiment.

2.3. Analytical Procedures. The concentration of the aroma compounds was analyzed in the permeate, retentate, and feed streams by gas chromatography as described in Alvarez et al.¹⁸ Apple juice concentration was measured by an Abbe refractometer (Sibuya Optical, Tokyo, Japan) and expressed as degrees Brix. Density and viscosity were determined by an Anton-Paar DMA-35 model (Graz, Ostrich) digital densimeter

and a Cannon-Fenske (Afora, Barcelona, Spain) viscosimeter, respectively.

3. The Model

To predict permeate flux and aroma compounds retention, the *preferential sorption-capillary flow* model, described by Sourirajan et al.,^{13,14,16} was used. An adaptation of this model to artificial solutions simulating apple juice was thoroughly described in a previous paper by the authors.¹⁸ The equations describing solute and solvent flux are the following:

$$N_A = \frac{D_{AM}}{K\delta}(C_{A2} - C_{A3}) \quad (1)$$

$$N_B = A(\Delta P - \Delta \Pi) \quad (2)$$

where N_A and N_B are the flux of solute and solvent, respectively, through the membrane, A is the solvent permeability of the membrane, ΔP is the pressure difference across the membrane, $\Delta \Pi$ is the osmotic pressure difference at both sides of the membrane, C_{A2} and C_{A3} are the solute concentration on the membrane surface at the feed side and at the permeate side, respectively, and $D_{AM}/K\delta$ is the solute transport parameter, which is usually treated as an unknown parameter.

The concentration of solute on the membrane surface at the feed side was estimated by the film theory

$$N_A + N_B = k_A C_1 \ln \left(\frac{X_{A2} - X_{A3}}{X_{A1} - X_{A3}} \right) \quad (3)$$

where k_A is the mass-transfer coefficient, C_1 is the molar density of the bulk solution, and X_{A1} , X_{A2} , and X_{A3} are the molar fractions of the solute in the bulk solution and on the membrane surface at the feed and permeate sides, respectively. Because solute flux through the membrane is very small compared to solvent flux, N_A can be overlooked in eq 3, so that

$$X_{A2} = X_{A3} + (X_{A1} - X_{A3}) \exp(N_B/k_A C_1) \quad (4)$$

The mole fraction of the solute in the permeate was calculated as

$$X_{A3} = \frac{N_A}{N_A + N_B} \approx \frac{N_A}{N_B} \quad (5)$$

Retention of the aroma compounds (R) was calculated by the following equation:

$$R(\%) = \left(1 - \frac{C_{A3}}{C_{A1}} \right) \times 100 \quad (6)$$

The procedure followed to estimate permeate flux and aroma compounds retention was the same as that previously described.¹⁸

3.1. Prediction of Permeate Flux. According to the *preferential sorption-capillary flow* model, solvent flux through the membrane is defined by eq 2. The pure water permeability coefficient, A , was determined from experiments with distilled water conducted at different TMPs.

The estimation of water permeability of the MSCB 2521 R99 membrane was carried out in a previous work¹⁸ and led to the following expression to describe

the influence of temperature and feed flow on the permeability:

$$A_{Q,T} = 32.186(t/25)^{0.62}(Q/400)^{-0.1447} \quad (7)$$

where A is the permeability in L/h·m²·MPa, t the temperature in °C, and Q the feed flow in L/h.

The variation of permeability with feed flow was explained as a consequence of the pressure drop inside the membrane module.¹⁸

The estimation of the water permeability of the MSCE 4040 R99 membrane will be described in the Results and Discussion section.

The osmotic pressure was considered to be due to the different concentrations of solutes at both sides of the membrane:

$$\Delta \Pi = \Pi(C_{A2}) - \Pi(C_{A3}) \quad (8)$$

Because the concentration of the permeate (C_3) is very low, it can be rejected in this equation. Taking into account their high concentration and low molecular weight, sugars and organic acids were considered to be the major constituents of apple juice contributing to osmotic pressure. The molecular weight and concentration of these compounds in the apple juice used in this work are shown in Table 1.

The estimation of the osmotic pressure due to glucose and sucrose was carried out by means of an empirical equation obtained by Nabetani et al. (1992).¹⁹ In this work, it has been supposed that fructose and sorbitol behave in the same way as glucose regarding their contribution to osmotic pressure. In fact, both compounds have chemical composition and molecular weight similar to those of glucose. To estimate the osmotic pressure due to malic acid, the van't Hoff equation was considered. This equation implies acceptance of several simplifications, and it differs greatly from experimental data at high concentrations. However, it can be employed for diluted solutions of concentration lower than 1%, as is the case of malic acid in apple juice.²² Therefore, the osmotic pressure at the membrane surface was estimated by the following equation:

$$\Pi(C_{s2}, C_{g2}, C_{m2}) = - \frac{RT}{V_w} \ln \left[\frac{(1000 - C_{s2} - C_{sg2})/M_w - 4C_{s2}/M_s - 2C_{g2}/M_g}{(1000 - C_{s2} - C_{s2})/M_w - 3C_{s2}/M_s - C_{g2}/M_g} \right] + RT \frac{C_{m2}}{M_m} \quad (9)$$

where C_{s2} , C_{g2} , and C_{m2} represent the concentrations of sucrose, glucose, and malic acid, respectively, at the membrane surface, expressed in kg/m³; M_s , M_g , and M_m represent respectively their molecular weights; M_w is the molecular weight of water; R is the universal gas constant; T is the absolute temperature; and V_w is the molar volume of pure water (18.07×10^{-3} m³/kmol).

The estimation of the concentration of the solutes on the membrane surface was made using the film theory:

$$C_{A2} = C_{A1} \exp(N_B/k_A C_1) \quad (10)$$

The mass-transfer coefficient of the solutes (k_A) was estimated using Schock and Miquel's correlation,²³ as described in Alvarez et al.:¹⁸

$$Sh = 0.065 Re^{0.875} Sc^{0.25} \quad (11)$$

where Sh is the Sherwood number, Re is the Reynolds number, and Sc is the Schmidt number. This correlation was established for spiral wound modules and Reynolds numbers in the range of $100 < Re < 1000$. The tangential flow velocity was calculated as previously described.^{18,23}

The apple juice density (ρ) and viscosity (μ) in the boundary layer were estimated as a function of concentration and temperature, using respectively two empirical equations proposed by Constela et al. (1989).²¹ These equations were tested with the apple juice employed as the feed solution in this work, and the predicted results were in agreement with the experimental measurements

$$\rho = 0.8272 + 0.34708 \exp(0.01 C) - 5.479 \times 10^{-4} T \quad (12)$$

$$\ln \frac{\mu}{\mu_w} = \frac{aC}{(100 - bC)} \quad (13)$$

with $a = -0.25801 + 817.11/T$ and $b = (1.8909 - 3.0212) \times 10^{-3} T$, where μ_w is the viscosity of water at the same temperature and C is the concentration in °Brix.

The concentration of solutes in the boundary layer was considered as the mean value between their concentration in the feed solution and that at the membrane surface.

The diffusion coefficients of glucose and sucrose in the boundary layer were estimated using the equation proposed by Gladen and Dole¹⁹ for aqueous binary solutions containing glucose and sucrose:

$$D_i = D_{oi}(\mu_w/\mu)^{0.45} \quad (14)$$

where the subscript i refers to glucose or sucrose, D_i is their diffusion coefficient in the boundary layer, and D_{oi} is their diffusion coefficient in a very dilute solution. The values of D_{oi} for glucose and sucrose from the literature²⁴ at 25 °C are 6.9×10^{-10} and 5.24×10^{-10} m²/s, respectively. In this work this equation was also considered to be valid for malic acid. The value of D_{oi} for malic acid was estimated using the equation of Wilke–Chang:²⁵

$$D_{AB} = \frac{117.3 \times 10^{-8} (\Phi M_B)^{0.5} T}{\mu V_{bp,A}^{0.6}} \quad (15)$$

where D_{AB} is the diffusion coefficient of a solute A in a solvent B expressed in m²/s, M_B is the molecular weight of the solvent (kg/kmol), $V_{bp,A}$ is the molar volume of the solute at its normal boiling point (m³/kmol), and Φ is an associated parameter of the solvent, whose value is 2.6 for water. This equation was also used to estimate the value of the diffusivity at other temperatures:

$$D_{AB1} = \frac{D_{AB2} \mu_2 T_1}{\mu_1 T_2} \quad (16)$$

where subscripts 1 and 2 refer to two different temperatures.

To estimate the values of k_A , ρ , μ , and D_{AB} in the boundary layer, the concentration of the solutes at the membrane surface, C_{A2} , must be known. Therefore, to

Table 3. Experimental Value of $D_{AM}/K\delta$ at 25 °C

compound	$D_{AM}/K\delta$ at 25 °C (cm/s $\times 10^4$)
ethyl acetate	4.818
trans-2-hexenal	4.574
hexanal	2.084
butanol	1.905
ethyl butanoate	1.739
hexyl acetate	1.564
hexanol	1.556
isopentyl acetate	0.387
isobutanol	0.302
isopentanol	0.297
ethyl-2-methyl butanoate	0.223

predict the value of permeate flux, N_B , it is necessary to simultaneously solve not only eqs 2, 9, and 10 but also eqs 11–13 and 15.

3.2. Prediction of Aroma Compounds Retention.

Equation 1 describes the flux of the solutes through the membrane:

$$N_A = \frac{D_{AM}}{K\delta} (C_{A2} - C_{A3}) = \frac{D_{AM}}{K\delta} (C_2 X_{A2} - C_3 X_{A3}) \quad (1)$$

where subscript A refers to each aroma compound in the apple juice and C_2 and C_3 are the molar densities of the solution on the membrane surface and in the permeate, respectively. The molar density C_2 was estimated from the literature²⁴ as a function of glucose, sucrose, and malic acid concentrations on the membrane surface (C_{g2} , C_{s2} , and C_{m2}), previously calculated. The molar density of the permeate was considered to be equal to that of water at the same temperature.

The solute transport parameters of the aroma compound were determined in a previous work¹⁸ for the MSCB 2521 R99 membrane. Table 3 shows these values at 25 °C, and eq 17 describes the influence of the temperature on this parameter. The solute transport parameter was observed to be independent of the feed flow and TMP

$$\left(\frac{D_{AM}}{K\delta} \right) = \left(\frac{D_{AM}}{K\delta} \right)_{\text{ref}} e^{0.098(T - T_{\text{ref}})} \quad (17)$$

with T_{ref} being the reference temperature of 25 °C. This equation was obtained for a temperature range of 15 °C $\leq T \leq 30$ °C.

The solute transport parameter is a function of the membrane and solute nature.¹⁶ Because both spiral wound membrane modules are constituted of the same type of PA membrane, the solute transport parameter of each solute was considered to be the same for both membrane modules.

The molar fractions of the aroma compounds at the membrane surface and in the permeate stream were estimated by means of eqs 4 and 5, respectively. To estimate the mass-transfer coefficient of each aroma compound, eq 11 was used. The following equation, proposed by Chandrasekaran and King,²⁰ was considered to estimate the diffusion coefficients of the aroma compounds in the concentration polarization boundary layer:

$$\log(D_A/D_{oA}) = 4.61 \log C_w - 8.04 \quad (18)$$

with D_A and D_{oA} being the diffusion coefficients of the aroma compounds in the boundary layer and in a diluted aqueous solution at 25 °C, respectively, and C_w

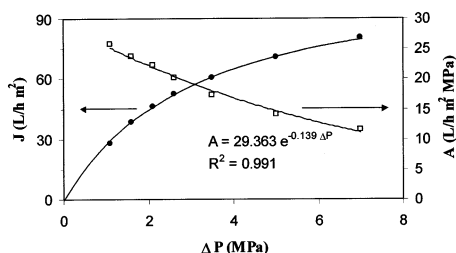


Figure 2. Influence of TMP on pure water flux and permeability at a temperature of 25 °C and a feed flow of 4200 L/h for the MSCE 4040 R99 membrane.

the concentration of water in the boundary layer in mol/L. This is an empirical equation that is valid for estimating the diffusivity of diluted organic compounds in aqueous solutions of sugars (glucose, fructose, and sucrose, individually as well as mixed). Because these sugars represent 93% of the solutes of the apple juice used in this work, it was considered that this equation can also be used to predict the value of the diffusion coefficients of the aroma compounds in apple juice. The diffusion coefficient of each aroma in a dilute aqueous solution at 25 °C was obtained from the literature.^{26–28} For those compounds whose diffusion coefficients were not available, the empirical equation of Wilke–Chang (eq 15) was used. The value of the diffusion coefficients at temperatures other than 25 °C was determined using eq 16.

When the system formed by eqs 1, 4, and 5 is solved, the values of N_A , X_{A2} , and X_{A3} for each aroma compound were obtained. Finally, rejection was calculated by eq 6.

4. Results and Discussion

4.1. Determination of MSCE 4040 R99 Membrane Permeability. The pure water permeability coefficient of the MSCE 4040 R99 membrane was determined from experiments with distilled water as previously described in section 3.1. In Figure 2 flux and permeability were plotted versus TMP. It can be observed that permeability decreases exponentially with TMP. Other authors found the same relationship between A and TMP using different types of membranes and experimental conditions, and they explained the reduction of A with pressure as a consequence of membrane compaction. Sourirajan and Matsuura proposed the following correlation between both variables:¹⁶

$$A = A_0 \exp(-\alpha \Delta P) \quad (19)$$

where α is a measure of the susceptibility of the membrane for compaction under pressure and A_0 is a constant that represents the permeability of a membrane that does not suffer compaction.

However, the reduction of permeability with TMP was not observed at laboratory scale,¹⁸ where a linear relationship between flux and TMP was found. This is probably due to the lower pressures considered when using the MSCB 2521 R99 membrane module.

An increase in permeability with temperature was also observed, as can be noted from Figure 3. The increase in permeability with temperature can be related to the reduction of pure water viscosity with this variable.

4.2. Concentration of Apple Juice at Laboratory Scale. Experiments were carried out at different TMPs

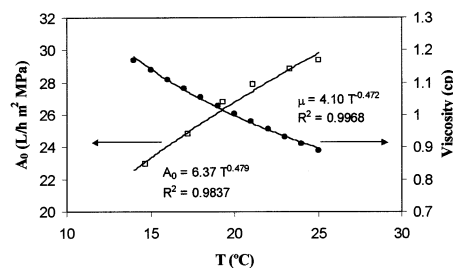


Figure 3. Influence of temperature on pure water viscosity and permeability through the MSCE 4040 R99 membrane.

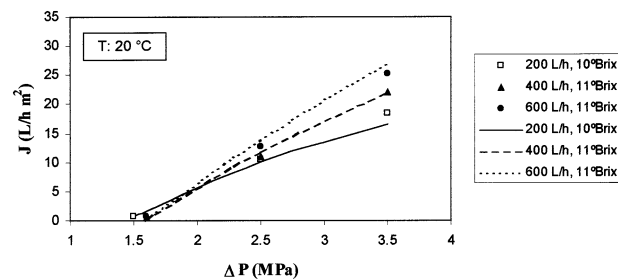


Figure 4. Experimental (symbols) and predicted (lines) permeate flux at different TMPs and feed flows.

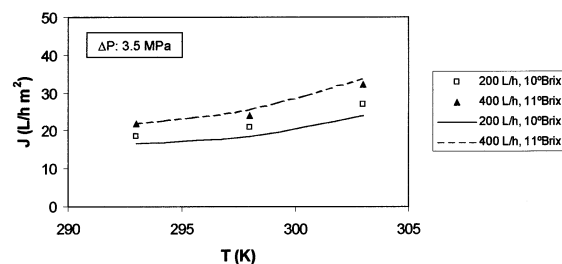


Figure 5. Experimental (symbols) and predicted (lines) permeate flux at different temperatures and feed flows.

(1.5–3.5 MPa), temperatures (20–30 °C), and feed flow rates (200–600 L/h). The corresponding Reynolds numbers ranged between 52 and 220. Permeate flux and aroma compounds retention were measured and the experimental results compared with the data predicted by the model.

Figures 4 and 5 display permeate flux as a function of TMP and temperature, respectively, at different feed flows. The lines represent the values predicted by the model and the symbols the experimental values. It can be observed that permeate flux increases with feed flow, TMP, and temperature, as expected, because of the increase in membrane permeability with temperature; because of the better mixing in the high-pressure channel when feed flow increases, thus reducing the concentration polarization phenomena; and because TMP is the driving force for the RO process, as can be observed from eq 1.

The experiments at 200 L/h feed flow were carried out with 10 °Brix apple juice, while the rest of the experiments were performed with 11 °Brix apple juice. When working at high TMPs, it was observed that the permeate flux obtained at 200 L/h was lower than the permeate flux at 400 and 600 L/h, even though the feed concentration was lower. However, when operating at low TMPs, the effect of the increase in the osmotic pressure due to an increase in the feed concentration becomes more important. The influence of the feed flow on permeate flux is greater at higher TMPs, as observed by other authors^{11,22} using different membranes and feed solutions.

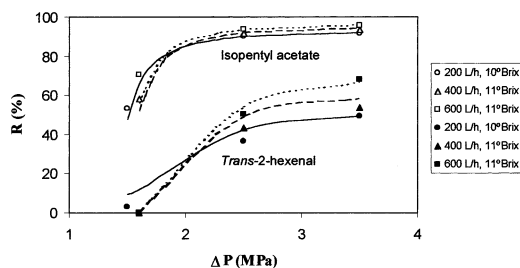


Figure 6. Experimental (symbols) and predicted (lines) retention at different TMPs and feed flows (temperature 20 °C).

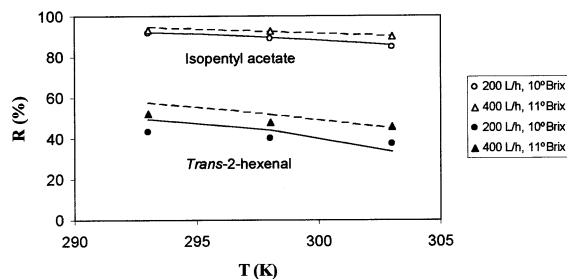


Figure 7. Experimental (symbols) and predicted (lines) retention at different temperatures and feed flows (TMP: 3.5 MPa).

A good agreement between experimental and calculated fluxes was observed. Differences between experimental and calculated data were around 5% for most cases, while the highest discrepancy observed was 15%. The model predicts slightly lower permeate fluxes than experimental ones at 200 L/h and slightly higher fluxes at 600 L/h. The worst fit was obtained at 200 L/h feed flow. The reason for this discrepancy could be due to the fact that, operating at 200 L/h, permeate flow is not negligible when compared to feed flow. Therefore, both the feed concentration and flow change from the inlet to the outlet of the membrane. An average value of both parameters was considered for the calculations. However, the variation of both variables inside the module is not known and, probably, not linear. This effect is less important for the other feed flows considered (400 and 600 L/h). Moreover, Schock and Miquel's correlation²³ used to estimate the mass-transfer coefficients was proven for Reynolds numbers between 100 and 1000. When working at 200 L/h, the Reynolds numbers were lower than 100. At 400 and 600 L/h, a much better fit was found. The agreement between experimental and calculated fluxes is very similar to that obtained for artificial solutions simulating apple juice,¹⁸ thus confirming the validity of the assumptions considered.

Figures 6 and 7 compare experimental and predicted retention for isopentyl acetate and *trans*-2-hexenal, which are the compounds that show the best and worst agreement, respectively, between experimental and calculated values. It can be observed that retention increases with TMP and feed flow but decreases with temperature. When operating at higher TMPs, the transport of solutes toward the membrane surface increases, thus increasing solute flux through the membrane. The reason retention increases with TMP is the increase in solvent flux with this variable. At the operating conditions considered in this work, solvent flux is more affected by pressure than solute flux, so that, when TMP increases, the N_B/N_A ratio is higher. It can also be observed that the effect of pressure on retention is higher when operating at low pressures. At high TMPs, however, the influence of this variable on retention is much lower.

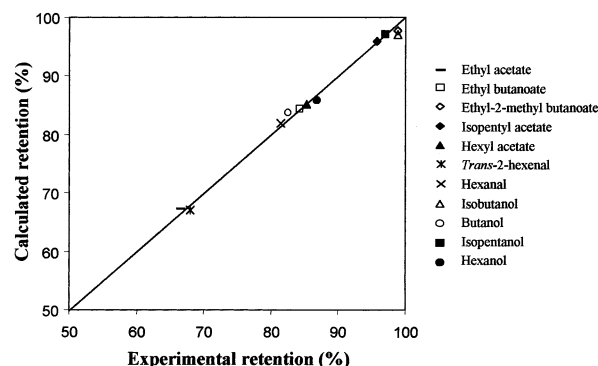


Figure 8. Comparison between experimental and predicted aroma compounds retention at 11 °Brix apple juice concentration, 20 °C, 3.5 MPa, and 600 L/h.

The increase of retention with feed flow can be explained as a result of the reduction of the solute concentration on the membrane surface when feed flow rises, thus decreasing solute permeation. Moreover, permeate flux increases with this variable. The reduction of solute retention with temperature can be due to the exponential increase of the solute transport parameter with this variable. For some of the compounds, the reduction of retention was as high as 40% when the temperature was raised from 20 to 30 °C.

A good agreement was also observed between experimental and calculated retention. The worst fit was obtained for TMPs lower than 1.7 MPa. At such low TMPs, the model predicts very low, close to zero, permeate fluxes, while the experimental values were slightly higher. In this case, small variations in permeate flux strongly affect the N_B/N_A ratio and, hence, the retention. Therefore, small errors in measuring the TMP, arising from the pressure meter or from the unknown variation of TMP along the membrane module, can affect the results predicted by the model. Nevertheless, from a practical point of view, working at very low TMPs, which also leads to very low permeate fluxes, is not of interest, and higher pressures will be necessary when operating a plant. At these pressures the model fits well with the experimental data for all of the compounds, as can be observed from Figure 8. Differences between experimental and calculated retention were around 5% for most of the aroma compounds and operating conditions studied. The best agreement was obtained for the compounds that show the highest retention, while the compounds with low retention (ethyl acetate and *trans*-2-hexenal) show the highest divergence, which, for certain operating conditions, was higher than 10%. The same trend had been previously observed with artificial solutions.¹⁸ For certain operating conditions, the agreement between experimental and predicted retention was slightly worse than the one observed with model solutions, probably because of the higher number of assumptions considered. Moreover, the errors of the analytical methods were higher when using apple juice. Another possible source of error is membrane fouling, which was not taken into account and could affect aroma compounds permeation. Fouling is expected to be higher when using apple juice as the feed solution than when using glucose and aroma solutions. However, differences between calculated and predicted data are fairly low and quite similar to the ones observed with artificial solutions for most of the compounds and operating conditions. Therefore, it is justified not to take into consideration membrane foul-

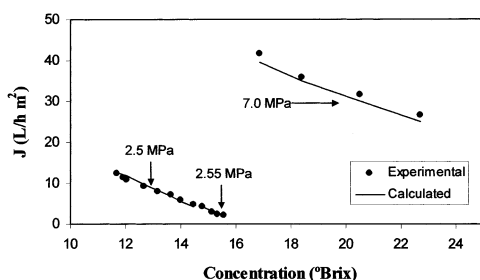


Figure 9. Experimental and predicted permeate flux as a function of concentration and TMP when concentrating apple juice at pilot-plant scale (temperature 25 °C; feed flow 4200 L/h).

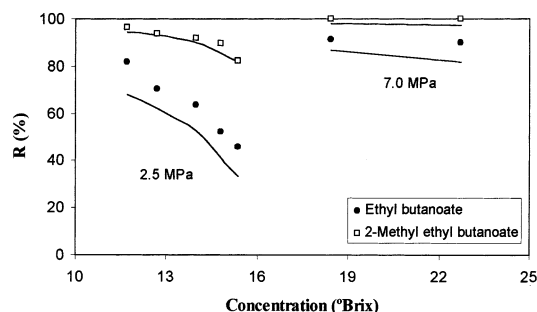


Figure 10. Experimental and predicted retention as a function of concentration and TMP when concentrating apple juice at pilot-plant scale (temperature 25 °C; feed flow 4200 L/h).

ing. In fact, for most of the RO processes, the concentration polarization phenomenon is more important than fouling.¹¹ Moreover, the model describes the effect of operating variables on flux and retention reasonably well.

4.3. Concentration of Apple Juice at Pilot-Plant Scale. Experiments were carried out at 2.5 and 7.0 MPa TMPs, a temperature of 25 °C, and a feed flow of 4200 L/h, and apple juice was concentrated from 11.7 to 22.7 °Brix. The corresponding Reynolds numbers ranged between 323 and 487.

Figure 9 compares experimental permeate flux with the data predicted by the model. Permeate flux was observed to increase with TMP and decrease with the feed concentration because of the increase of the osmotic pressure. It can be noted that the maximum concentration that can be reached is dependent on the TMP considered. When operating at 7.0 MPa, it is possible to concentrate the apple juice over 22 °Brix with permeate fluxes higher than 25 L/h·m². A good agreement between experimental and calculated fluxes was also observed at pilot-plant scale, where a mean divergence of about 6% between both data was obtained.

Figure 10 displays experimental and predicted retention for ethyl-2-methyl butanoate and ethyl butanoate, which are the compounds that show the best and worst agreement, respectively, between experimental and calculated values. It can be observed that retention decreases with the feed concentration. An increase in the feed concentration involves an increase in the viscosity and density of the solution on the membrane surface. Thus, the mass-transfer coefficient of the aroma compounds is lower, and their concentration on the membrane surface and their permeation increase. Moreover, solvent flux decreases with concentration, so that the N_B/N_A ratio, and hence the retention, also decreases with this variable. It can also be observed that retention increases a great deal when the pressure is raised from 2.5 to 7.0 MPa, even though the concentration is higher.

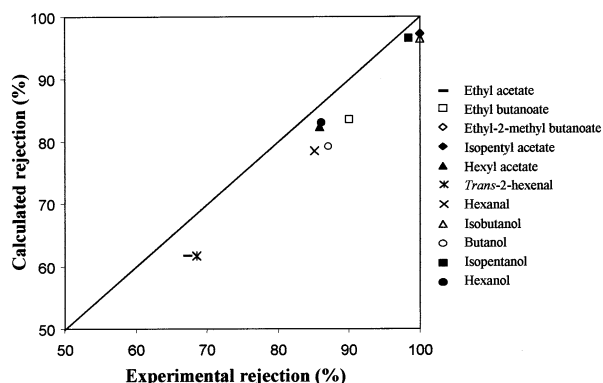


Figure 11. Comparison between experimental and predicted aroma compounds retention at 22.7 °Brix apple juice concentration, 25 °C, 7.0 MPa, and 4200 L/h for the MSCE 4040 R99 membrane.

At 7.0 MPa retention is higher than 60% for all of the compounds, even when the concentration is as high as 22.7 °Brix, as can be observed from Figure 11. In addition, retention is higher than 80% for all of the compounds except ethyl acetate (which was negatively related to apple juice flavor by some authors^{6,7}) and *trans*-2-hexenal.

The discrepancy between calculated and experimental retention is higher than that observed at laboratory scale. Differences were observed to be higher at 2.5 MPa than at 7.0 MPa and were also higher for the compounds that show the lowest retention. A mean divergence of about 15% was obtained, but for certain compounds and operating conditions, it was as high as 25%. The model predicts lower retention than the experimental one for all of the aroma compounds and operating conditions tested. It is possible that the solute transport parameters are lower for the MSCE 4040 R99 membrane than for the MSCB 2521 R99 membrane, just as water permeability was observed to be lower. In fact, the pure water flux through the pilot-scale membrane was about 20% lower than that indicated by the manufacturer, and the same could happen with the solute fluxes.

Taking into account these results, it is recommended to operate at high TMPs and feed flows because higher permeate fluxes and aroma retentions are obtained. Moreover, the maximum concentration that can be reached also increases with TMP. To avoid losses and alterations of the aroma, a low-temperature operation is recommended. However, permeate flux decreases with temperature, so that a compromise solution must be considered. When operating at 7.0 MPa TMP, 4200 L/h feed flow, and 25 °C temperature, concentrations higher than 22 °Brix can be reached with high permeate fluxes (higher than 25 L/h·m²) and high solute retention (higher than 80% for most of the compounds).

5. Conclusions

The *preferential sorption-capillary flow* model describes reasonably well the experimental data on permeate flux and aroma compounds rejection during the RO concentration of apple juice using MSCB 2521 R99 and MSCE 4040 R99 membranes.

Permeate flux and rejection were observed to increase with TMP and feed flow and to decrease with concentration, while permeate flux increased with temperature and retention decreased with this variable in the range of operating conditions tested. At laboratory scale, permeate flux and retention were accurate to within 5%

for most of the aroma compounds and operating conditions considered. The worst fit was noted for the experiments conducted at 200 L/h and for the aroma compounds showing the lowest retention. Discrepancies between experimental and predicted data were very similar to those obtained in a previous work using artificial solutions simulating apple juice, thus demonstrating the validity of the assumptions and correlations considered.

At pilot-plant scale, a mean divergence of about 6% between experimental and calculated permeate fluxes was observed. However, the model predicted a lower retention than the experimental one for all of the compounds and operating conditions considered. A mean divergence between the experimental and calculated retention of about 15% was obtained, but for the compounds that show the lowest retention and for certain operating conditions, it was as high as 25%. The discrepancy between the experimental and calculated retention at pilot-plant scale was higher than the one observed at laboratory scale.

The proposed model is able to predict the influence of operating conditions on permeate flux and retention and so can be used to optimize the operating variables. Taking the influence of operating conditions on permeate flux and retention into account, it is recommended to operate at high TMPs and feed flows and at moderate temperatures. When operating at 7.0 MPa TMP, 4200 L/h feed flow, and 25 °C temperature, concentrations higher than 22 °Brix can be reached with high permeate fluxes (higher than 25 L/h·m²) and high solute retention (higher than 80% for most of the compounds). These results suggest that RO can be successfully used for the preconcentration of apple juice because high-quality apple juice is obtained with high permeate flux.

Acknowledgment

This work was supported by the EU (European Union) through the AAIR Project PL94-1931 and by the MEC (Ministerio de Educación y Ciencia, Spain). The authors also thank the apple processing factory Valle, Ballina and Fernández, S.A., for the apple juice and apple aroma concentrate supplied.

List of Symbols

A = solvent permeability of the membrane, kmol/s·m²·MPa
 A_0 = solvent permeability of a membrane that does not suffer compaction, kmol/s·m²·MPa
 a = coefficient in eq 15
 b = coefficient in eq 15
 C = concentration, kmol/m
 D = diffusion coefficient, m²/s
 $D_{AM}/K\delta$ = solute transport parameter, m/s
 d_h = equivalent hydraulic diameter, m
 J = flux through the membrane, m/s
 k = mass-transfer coefficient, m/s
 M = molecular weight, kg/kmol
 N = flux through the membrane, kmol/s·m²
 ΔP = transmembrane pressure, MPa
 Q = feed flow, m³/s
 R = retention, %
 R = universal gas constant, MPa·m³/K·kmol
 Re = Reynolds number ($d_h v \rho / \mu$)
 Sc = Schmidt number ($\mu / \rho D_A$)
 Sh = Sherwood number ($k_A d_h / D_A$)
 t = temperature, °C
 T = absolute temperature, K

v = tangential flow velocity, m/s

V = molar volume, m³/kmol

X = mole fraction

Greek Letters

α = susceptibility of the membrane for compaction under pressure

Φ = associated parameter of the solvent in the equation of Wilke–Chang

μ = solution viscosity, kg/m·s

Π = osmotic pressure, MPa

ρ = solution density, kg/m³

Subscripts

A = solute

B = solvent

bp = boiling point

g = glucose

m = malic acid

o = very dilute solution

ref = reference

s = sucrose

w = water

1 = bulk solution

2 = membrane surface at feed side

3 = permeate

Literature Cited

- (1) Sheu, M. J.; Wiley, R. C. Preconcentration of Apple Juice by Reverse Osmosis. *J. Food Sci.* **1983**, 48, 422.
- (2) Rao, M. A. Concentration of Apple Juice. In *Processed Apple Products*; Downing, D. L., Ed.; Van Nostrand Reinhold: New York, 1989.
- (3) Scott, K. *Handbook of industrial membranes*; Elsevier: Oxford, 1995.
- (4) Álvarez, S.; Riera, F. A.; Álvarez, R.; Coca, J. Permeation of Apple Juice Aroma Compounds in Reverse Osmosis. *Sep. Purif. Technol.* **1998**, 14, 209.
- (5) Merson, R. L.; Morgan, J. A. I. Juice Concentration by Reverse Osmosis. *Food Technol.* **1968**, 22, 631.
- (6) Flath, R. A.; Black, D. R.; Guadagni, D. G.; McFadden, W. H.; Schultz, T. H. Identification and Organoleptic Evaluation of Compounds in Delicious Apple Essence. *J. Agric. Food Chem.* **1967**, 15, 29.
- (7) Durr, P.; Rothlin, H. Development of a Synthetic Apple Juice Odor. *Lebensm.-Wiss. Technol.* **1981**, 14, 313.
- (8) Pepper, D.; Orchard, A. C. J.; Merry, A. J. Concentration of Tomato Juice and Other Fruit Juices by Reverse Osmosis. *Desalination* **1985**, 53, 157.
- (9) Chua, H. T.; Rao, M. A.; Acree, T. E.; Cunningham, D. G. Reverse Osmosis Concentration of Apple Juice: Flux and Flavor Retention by Cellulose Acetate and Polyamide Membranes. *J. Food Process Eng.* **1987**, 9, 231.
- (10) Walter, J. B. Reverse Osmosis Concentration of Juice Products with Improved Flavor. U.S. Patent 4959237, Sept 25, 1990.
- (11) Álvarez, V.; Álvarez, S.; Riera, F. A.; Álvarez, R. Permeate Flux Prediction in Apple Juice Concentration by Reverse Osmosis. *J. Membr. Sci.* **1997**, 127, 25.
- (12) Soltanieh, M.; Gill, W. N. Review of Reverse Osmosis Membrane and Transport Models. *Chem. Eng. Commun.* **1981**, 12, 279.
- (13) Kimura, S.; Sourirajan, S. Analysis of Data in Reverse Osmosis with Porous Cellulose Acetate Membranes Used. *AIChE J.* **1967**, 13, 497.
- (14) Agrawal, J. P.; Sourirajan, S. Reverse Osmosis, Flow through Porous Media Symposium. *Ind. Eng. Chem.* **1969**, 61, 62.
- (15) Malalyandl, P.; Matsuura, T.; Sourirajan, S. Predictability of membrane performance for mixed solute reverse osmosis systems. System cellulose acetate membrane–D-glucose–D,L-malic acid–water. *Ind. Eng. Chem. Process Des. Dev.* **1982**, 21, 227.
- (16) Sourirajan, S.; Matsuura, T. *Reverse Osmosis/Ultrafiltration Principles*; National Research Council Canada Publications: Ottawa, 1985.

- (17) Dickson, J. M.; Whitacker, G.; DeLeeuw, J.; Spencer, J. Dilute single and mixed solute systems in a spiral wound reverse osmosis module. Part II. Experimental data and application of the model. *Desalination* **1994**, *99*, 1.
- (18) Álvarez, S.; Riera, F. A.; Álvarez, R.; Coca, J. Prediction of flux and aroma compounds rejection in a reverse osmosis concentration of apple juice model solutions. *Ind. Eng. Chem. Res.* **2001**, *40*, 4925–4934.
- (19) Nabetani, H.; Nakajima, M.; Watanabe, A.; Nakao, S.; Kimura, S. Prediction of the flux for the reverse osmosis of solutions containing sucrose and glucose. *J. Chem. Eng. Jpn.* **1992**, *25*, 575.
- (20) Chandrasekaran, S. K.; King, C. Multicomponent Diffusion and Vapor–Liquid Equilibria of Dilute Organic Components in Aqueous Sugar Solutions. *AIChE J.* **1972**, *18*, 513.
- (21) Constela, D. T.; Lozano, J. E.; Crapista, G. H. Thermophysical Properties of Clarified Apple Juice as a Function of Concentration and Temperature. *J. Food Sci.* **1989**, *54*, 663.
- (22) Cheryan, M. *Ultrafiltration and microfiltration handbook*; Technomic Pub.: Lancaster, PA, 1998.
- (23) Schock, G.; Miquel, A. Mass Transfer and Pressure Loss in Spiral Wound Modules. *Desalination* **1987**, *64*, 339.
- (24) Weast, R. C.; Astle, M. J. *CRC Handbook of Chemistry and Physics*; CRC Press: Boca Raton, FL, 1981.
- (25) Wilke, C. R.; Chang, P. Correlation of Diffusion Coefficients in Dilute Solutions. *AIChE J.* **1955**, *1*, 264.
- (26) Reid, R. C.; Prausnitz, J. M.; Poling, B. E. *The Properties of Gases and Liquids*; McGraw-Hill: New York, 1987.
- (27) Frey, D. D.; King, C. J. Diffusion Coefficients of Acetates in Aqueous Sucrose Solutions. *J. Chem. Eng. Data* **1982**, *27*, 419.
- (28) Li, S. F. Y.; Ong, H. M. Infinite Dilution Diffusion Coefficients of Several Alcohols in Water. *J. Chem. Eng. Data.* **1990**, *35*, 136.

Received for review January 7, 2002
 Revised manuscript received July 22, 2002
 Accepted August 9, 2002

IE020013G